GLEX-2012.02.2.9x12368

LUNAR RADIO TELESCOPES: A STAGED APPROACH FOR LUNAR SCIENCE, HELIOPHYSICS, ASTROBIOLOGY, COSMOLOGY, AND EXPLORATION

Joseph Lazio[*]
Jet Propulsion Laboratory, California Institute of Technology, Pasadena, CA USA;
Joseph.Lazio@jpl.nasa.gov
Judd D. Bowman[*]
Arizona State University, Phoenix, AZ USA
Jack O. Burns[*]
University of Colorado at Boulder, Boulder, CO USA
W. M. Farrell[*]
NASA/Goddard Space Flight Center, Greenbelt, MD USA
D. L. Jones[*]
Jet Propulsion Laboratory, California Institute of Technology, Pasadena, CA USA
J. C. Kasper[*]
Harvard-Smithsonian Center for Astrophysics, Cambridge, MA USA
R. J. MacDowall[*]
NASA/Goddard Space Flight Center, Greenbelt, MD USA
K. P. Stewart[*]
Naval Research Laboratory, Washington, DC USA
K. Weiler[*]
Computational Physics, Inc., Washington, DC USA

Observations with radio telescopes address key problems in cosmology, astrobiology, heliophysics, and planetary science including the first light in the Universe (Cosmic Dawn), magnetic fields of extrasolar planets, particle acceleration mechanisms, and the lunar ionosphere. The Moon is a unique science platform because it allows access to radio frequencies that do not penetrate the Earth's ionosphere and because its far side is shielded from intense terrestrial emissions. The instrument packages and infrastructure needed for radio telescopes can be transported and deployed as part of Exploration activities, and the resulting science measurements may inform Exploration (e.g., measurements of lunar surface charging). An illustrative roadmap for the staged deployment of lunar radio telescopes is the following.

Stage Ia—One (or a few) antennas on an orbiter: The prime science is to detect the global cosmological signal from the (highly redshifted) hyperfine 21 cm transition of neutral hydrogen that is excited by the ultraviolet and X-ray radiation fields of the first stars and accreting black holes.

Stage Ib—One (or a few) antennas on the lunar surface: If on the near side, the antennas would monitor the lunar ionosphere and track the balance between solar wind-induced effects and interior outgassing of volatile gasses. If on the far side, the antennas would detect and begin studying the highly redshifted 21 cm signal. Deployment could be done either during sorties or telerobotically, and the science measurements from them would be a powerful probe of lunar surface charging. This stage could occur in parallel with Stage Ia.

Stage II—A small telescope on the near side: The prime science is to study particle acceleration within the inner heliosphere, and possibly in astrophysical sources. Such a telescope would be capable of detecting the magnetically generated emissions from solar system planets, and potentially from extrasolar planets. A target number of antennas would be 100, which could be deployed in an extended duration sortie or telerobotically.

Stage III—A large telescope on the far side: Such a telescope would be capable of studying the highly redshifted 21 cm signal from Cosmic Dawn and extending into the Dark Ages. It would also be capable of detecting the magnetospheric emission from extrasolar planets. A nominal number of antennas is 10^5, distributed over about ten kilometers. Deployment would be largely robotically, though possibly with astronaut oversight.

[*] NASA Lunar Science Institute

I. THE MOON AS A SCIENCE PLATFORM

Interest in placing a radio astronomical telescope on or around the Moon pre-dates the *Apollo* missions [1,2]. Two primary features of the lunar surface offer a significant benefit for astronomy at radio wavelengths, particularly at frequencies below 1000 MHz (wavelengths longer than 30 cm). Recognizing these features of a lunar surface radio telescope, a series of workshops and conferences have described preliminary concepts [3,4,5,6,7]. We emphasize that these advantages remain for astronomical observations at radio wavelengths, though recent analyses suggest that, at shorter wavelengths, free-space operations are likely to be superior [8].

I.I No Human-generated Interference

The majority of the integrated radio power emitted by our civilization is at frequencies below 150 MHz [9]. The FM radio band is at 88–107 MHz, and myriad other signals, both civil and military, are broadcast at these frequencies. At the Murchison Radio Observatory in Western Australia, a government-protected site that is hundreds of kilometers from the nearest major metropolitan area, several FM radio signals are persistently detected at the level of 3×10^{-24} W m^{-2} Hz^{-2} sr^{-1} due to reflections from meteors and aircraft [10,11,12,13]. This spectral flux density is only 1% of the dominant emitter in the sky (the integrated emission from the Milky Way Galaxy) and is orders of magnitude stronger than the typical radio astronomical object.

In contrast, the lunar far side is completely shielded from these intense terrestrial emissions. The Radio Astronomy Explorer-2 (RAE-2) and the *Apollo* Command Modules had radio systems that operated at frequencies below 1000 MHz. Both observed a complete cessation of terrestrial radio emission while in the radio quiet zone above the lunar far side [14]. Moreover, reflections of terrestrial interference from other spacecraft in view of the lunar far side (e.g., at the Sun-Earth L2 point) can be shown to be at a negligible level ($< 3 \times 10^{-33}$ W m^{-2} Hz^{-2} sr^{-1}).

I.II No (Permanent) Ionosphere

The refractive index of a fully or partially ionized medium (plasma) is a function of frequency and becomes negative below a characteristic *plasma frequency*. At frequencies below the plasma frequency, an electromagnetic wave is reflected upon incidence. The plasma frequency is $f_p \approx 9$ kHz $(n_e/1\ \mathrm{cm}^{-3})^{1/2}$.

For the Earth's ionosphere, typical electron densities result in plasma frequencies around 10 MHz, with the specific frequency depending upon a variety of conditions including solar activity and time of day. Observations near and below 10 MHz must be conducted from space, as the ionosphere is not transparent at these frequencies. More importantly, while the plasma frequency is around 10 MHz for the Earth's ionosphere, non-negligible absorption effects can appear at much higher frequencies, as high as 100 MHz [15], making sensitive observations from the ground problematic.

Finally, the combination of the ionosphere and distant terrestrial transmitters can scatter strong signals into the line of sight of a ground-based telescope, producing interference that would not otherwise be detectable. Because of ionospheric refraction, interference in the HF band (< 30 MHz) used for international communication is essentially independent of location on Earth. Reflections from ionized meteor trails are a well-known effect [e.g., 16], and such reflected interference is easily detectable by even modest radio telescopes [e.g., 17].

In contrast, while the Moon has a plasma layer due to solar irradiation during the lunar day, its density, and therefore its critical frequency, is much lower than that of Earth. The critical frequency is not expected to exceed 1 MHz, and typically is closer to 0.3 MHz (§II.III). Further, this ionized layer disappears during lunar night.

I.III Shielding from Solar Radio Emission

The Sun's proximity makes it the strongest celestial source at these frequencies when it is bursting. While this strength is advantageous for some of the science described below, in other cases, solar radio bursts are many orders of magnitude stronger than the signals of interest, most notably for highly redshifted neutral hydrogen signals from Cosmic Dawn and the Dark Ages. Within the solar system, the only mitigation for solar radio emissions is physical shielding. A free-flying mission could not be shielded from the solar radio emission (nor from human-generated terrestrial interference). Such shielding is readily accomplished by observing during lunar night and, while the same is true for the surface of the Earth, interference and ionospheric effects continue to occur during terrestrial night.

II. SCIENCE WITH RADIO FREQUENCY ANTENNAS ON THE LUNAR SURFACE

II.I Cosmic Dawn and the Dark Ages

Following recombination at a redshift $z \approx 1100$, about 370,000 years after the Big Bang, the Universe entered a largely neutral state in which the dominant baryonic component of the intergalactic medium (IGM) was neutral hydrogen (H I). By a redshift $z \sim 7$, about 1 billion years after the Big Bang, observations with a combination of ground- and space-based telescopes are showing that the precursors of modern-day galaxies existed and were beginning to re-ionize the surrounding H I [18,19, Fig. 1]; analysis of data

from the Wilkinson Microwave Anisotropy Probe (WMAP) suggests that the Reionization process is likely to have been an extended process, potentially beginning at $z \sim 12$, as early as a few hundred million years after the Big Bang [20]. Future observations with *James Webb Space Telescope* (JWST) and the Atacama Large Millimeter/Submillimeter Array (ALMA) have the potential to probe to $z \approx 15$–20, but only at radio wavelengths is there the likelihood of probing to earlier times.

The *New Worlds, New Horizons in Astronomy and Astrophysics* Decadal Survey, conducted by the U.S. National Research Council (NRC), highlighted the importance of obtaining measurements during this phase of the Universe by identifying "Cosmic Dawn" as one of the three science objectives guiding the science program for the 2010–2020 decade [21]. The Decadal Survey further identified the Epoch of Reionization as a science frontier discovery area with the opportunity for "transformational comprehension, i.e., discovery," and "What were the first objects to light up the Universe and when did they do it?" was identified as a frontier science question.

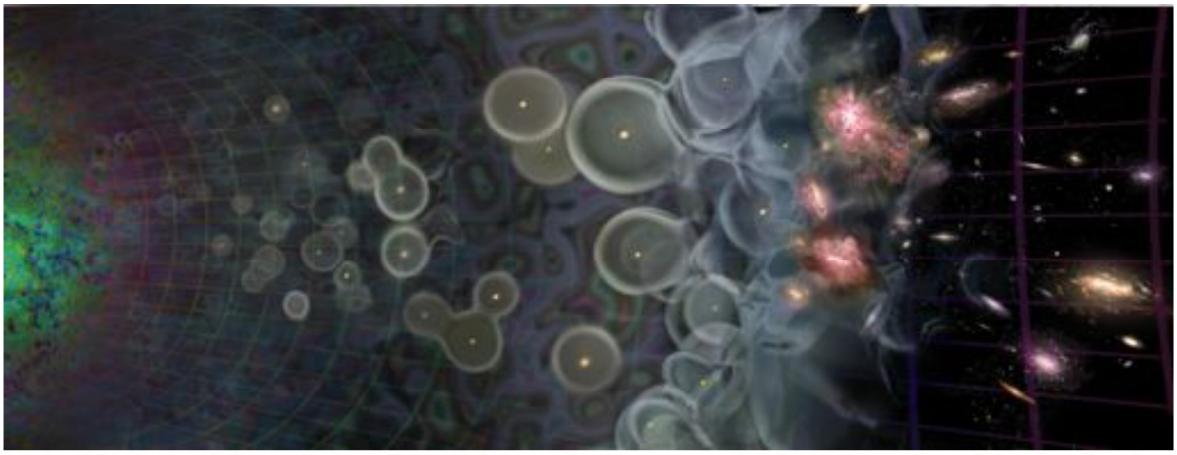

Fig. 1: Schematic of the evolution of the Universe. At the extreme left is the formation of the cosmic microwave background (CMB) approximately 370,000 years after the Big Bang, and at the extreme right is the current epoch, approximately 13.7 billion years after the Big Bang. Depicted is the formation of the first stars and the bubbles of ionized gas that their radiation carved into the surrounding neutral hydrogen, the gradual merging of those bubbles, and the formation of the first galaxies, leading to the largely ionized Universe of today. (Adapted from Loeb [22].)

The H I atom produces a spectral line at a frequency of 1420 MHz (wavelength of 21 cm) due to a hyperfine interaction between the angular momenta of the constituent proton and electron in the ground level energy state of the atom. This (redshifted) spin-flip (21 cm) hyperfine transition of H I presents a powerful means to track the influence of the first ionizing and heating sources on the IGM, potentially even tracing the evolution of the Universe before the first stars ignited.

Figure 2 shows the expected strength of the 21 cm H I line, relative to the CMB, over the redshift range of approximately 6–100 (≈ 15 million years to 1 billion years after the Big Bang), from when the excitation (spin) temperature of the H I transition tracks that of the gas kinetic temperature ($z \sim 100$) to the late times of Reionization ($z \sim 6$). During this time, the strength of the H I signal depends upon the temperature of the gas and the fraction of neutral hydrogen, quantities that both are affected by the time and rate at which the first ionizing and heating sources form.

The 21 cm intensity or brightness temperature of an IGM gas parcel at a redshift z, relative to the cosmic microwave background (CMB), is [24,25]

$$\delta T \approx 25 \text{ mK } x_{HI} (1 + \delta) [(1 + z)/10]^{1/2} \times [1 - T_{CMB}(z)/T_s] [H(z)/(1 + z)/dv_{\parallel}/dr_{\parallel}].$$

Here x_{HI} is the neutral fraction, δ is the fractional IGM overdensity in units of the mean, T_{CMB} is the CMB temperature, T_s is the spin (or excitation) temperature of this transition, $H(z)$ is the Hubble constant, and $dv_{\parallel}/dr_{\parallel}$ is the line-of-sight velocity gradient.

All four factors contain unique astrophysical information. The dependence on δ traces the development of cosmic structure, while the velocity gradient incorporates line-of-sight "redshift-space distortions" that separate aspects of the cosmological and astrophysical signals. The other two factors depend strongly on the ambient radiation fields in the early Universe: the ionizing background for x_{HI} and a

combination of the ultraviolet background (which mixes the 21 cm level populations through the Wouthuysen-Field effect) and the X-ray background (which heats the gas) for T_s.

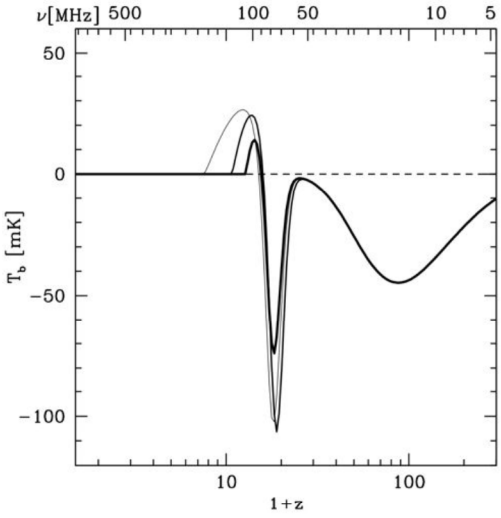

Fig. 2: Evolution of the 21 cm H I global signal, relative to the cosmic microwave background (CMB). The ordinate is the brightness temperature of the redshifted 21 cm signal, and the bottom (top) abscissa is the redshift (frequency, given the rest frame frequency of 1420 MHz). The thick black curve is a notional model, with the first star formation occurring at redshift $z \sim 30$, and in which the IGM is ionized by $z \sim 6$. Other curves illustrate a range of models for galaxy formation consistent with observational constraints [23]. Three epochs can be defined, the *Dark Ages* ($z \sim 30$–200), the *First Stars and Cosmic Dawn* ($z \sim 15$–30), and the *Epoch of Reionization* ($z \sim 6$–15).

Several epochs in the evolution of the H I signal can be identified, but these are currently essentially unconstrained by observations.

The Dark Ages ($z > 30$): Before the first stars and galaxies formed, the H I gas was influenced only by gas collisions and absorption of CMB photons. The gas cooled rapidly as the Universe expanded, and the resulting cold temperatures cause the 21 cm signal to appear in absorption. As the Universe expanded, the decreased gas density reduced the collision rate, and absorption of CMB photons drove the T_s into equilibrium with T_{CMB}. Consequently, the magnitude of the 21 cm absorption decreased and eventually disappeared by $z \sim 30$.

First Stars and Cosmic Dawn ($30 > z > 22$): Shortly thereafter, the first stars appeared ($z \sim 30$). Via the Wouthuysen-Field effect, the absorption and re-emission of their ultraviolet radiation drove T_s toward the kinetic temperature of the IGM gas, which remained well below T_{CMB} and resulted in a deep 21 cm absorption trough.

First Accreting Black Holes ($22 > z > 13$): Black holes likely formed at this time, e.g., as remnants from the first stars. Due to their intense gravity, gas falling into them would have been accelerated, shock heated, and begun to radiate X-rays. At this time, the IGM gas was extremely cold (~ 10 K), and the energetic X-ray photons from the accreting black holes began to heat it. This heating transformed the spin-flip signal from absorption into emission as the gas became hotter than the CMB.

Hot, Bubble Dominated Epoch ($13 > z > 6$): Also known as the Epoch of Reionization, once the gas became hot, the emission saturated, until photons from these stars and black holes started ionizing the gas in giant bubbles within the IGM. The rapid destruction of the neutral gas during Reionization then eroded the 21 cm signal.

Fully Ionized Universe ($z < 6$): Once the Epoch of Reionization completed and the neutral gas was destroyed, the 21 cm spin-flip signal disappeared.

There are two approaches for measuring the H I signal, which vary depending upon the assumed angular resolution and consequently the required sensitivity of the instrument or telescope [25,23,26].

II.I.I The Sky-Averaged 21 cm Signal

The sky-averaged 21 cm spectrum (Figure 2) is the most basic quantity of physical interest. Due to the cosmological redshift, each observed frequency corresponds to a different cosmic epoch, allowing the development of structure in the Universe to be traced. Figure 2 shows that the different eras identified in the previous section imprint distinct features—*Turning Points*—on the 21 cm spectrum. Crucially, our current understanding of the properties of the first galaxies and black holes is especially poor, with reasonable models providing variations over several orders of magnitude in their parameters. Pritchard & Loeb [27] built upon earlier models [28] to quantify the uncertainties and determine the relevant range of frequencies at which these features might occur.

The primary challenge in observing this sky-averaged background is separating the cosmological signal from the low radio frequency background. Harker et al. [29] have developed a detailed model of global signal observations accounting for instrumental effects, foregrounds, and the 21 cm signal. Applying a Markov-Chain Monte-Carlo (MCMC) algorithm, they explored the achievable bounds on

the positions of the signal turning points. This modeling is in the process of being tested against data from the Experiment to Detect the Global Epoch of Reionization Signal (EDGES) [30] and likely will form the basis for future, lower frequency observations, such as those around the Moon that we describe (§III).

II.I.II Fluctuations in the 21 cm Signal and Power Spectral Measurements

Complementing sky-averaged experiments are radio interferometric observations of 21 cm fluctuations. This approach allows one to measure the properties of individual structures, such as the ionized bubbles that fill the Universe during Reionization, either by mapping them or through their statistical properties. It is therefore much more powerful than the sky-averaged signal, but it is also much more difficult to measure because the signal from each structure is extraordinarily small. Experimental data is just starting to become available from the Precision Array to Probe the Epoch of Reionization (PAPER) [31] and the Giant Metrewave Radio Telescope (GMRT) [32] experiments, which will guide understanding of instrumental systematics in the future.

These measurements will constrain models of the first luminous sources to form in the Universe, and theoretical progress on predicting them has already informed work on the high-redshift Universe in other contexts. For example, the same ultraviolet radiation that excites the 21 cm signal also suppresses primordial star formation, so that observing the 21 cm signal helps us to understand the earliest phases of galaxy formation [33]. Recent theoretical work also underscores the need for observational constraints. Dalal et al. [34] predict that a velocity offset between gas and dark matter in the early Universe substantially delays structure formation, and it may dramatically amplify the 21 cm signal itself. Only measurements can distinguish among the competing theoretical predictions.

II.II Space Weather and Particle Acceleration

High-energy particle acceleration occurs in diverse astrophysical environments including the Sun and other stars, supernovae, black holes, and quasars. The mechanisms and sites of this acceleration remain poorly understood, in particular the roles of shock waves and magnetic reconnection. Within the inner heliosphere—an interval of 1–10 solar radii from the Sun—solar flares and coronal mass ejections (CMEs) are efficient particle accelerators.

Low radio frequency observations are an excellent remote diagnostic because electrons accelerated by these structures can produce intense radio bursts. The intensities of these bursts make them easy to detect, as well as providing information about the acceleration regions. The radio burst mechanisms discussed here involve emission at the local plasma frequency or its harmonics. (See also §II.III.) With a model for the electron density, the emission frequency can be converted into a height above the corona, and a changing frequency can be converted into radial speed.

Solar radio bursts are one of the primary remote signatures of electron acceleration in the inner heliosphere, and our focus is on two specific kinds, Type II and Type III radio bursts. Type II bursts originate from supra-thermal electrons ($E > 100$ eV) produced at shocks. These shocks generally are produced by CMEs as they expand into the heliosphere with Mach numbers greater than unity. Emission from a Type II burst drops slowly in frequency as the shock moves away from the Sun into lower density regions at speeds of 400–2000 km s^{-1}. Type III bursts are generated by fast (2–20 keV) electrons from magnetic reconnection. As the fast electrons escape at a significant fraction of the speed of light into the heliosphere along magnetic field lines, they produce emission that drops rapidly in frequency.

Electron densities in the inner heliosphere mean that the relevant radiation emission frequencies are below 10 MHz [35,36], and Bougeret et al. [38] present several examples that illustrate the active low radio frequency environment in space, as measured by the *non-imaging* WAVES instrument on the Wind spacecraft.[t]

Observations must be conducted from space because the ionosphere is opaque in this frequency range, and there are key questions that can only be addressed by an imaging instrument:

Acceleration at Shocks: Observations of CMEs near Earth suggest electron acceleration generally occurs where the shock normal is perpendicular to the magnetic field [38], similar to acceleration at planetary bow shocks and other astrophysical sites. This geometry may be unusual in the corona, where the magnetic field is largely radial. Geometric arguments suggest that the shocks at the front of CMEs generally have a quasi-parallel geometry (Q-||). Acceleration along the flanks of the CME, where the magnetic field-shock normal is quasi-perpendicular (Q-⊥) would seem to be a more likely location for the electron acceleration and Type II emission, but both Q-|| and Q-⊥ have been proposed as mechanisms for Type II emission [e.g., 39, 40].

Electron and Ion Acceleration: Observations at 2–15 MHz made with the Wind spacecraft showed

[t] For more recent work, see the SWAVES Web site, `http://swaves.gsfc.nasa.gov/`.

that complex Type III bursts (also called Type III-L) are highly correlated with CMEs and intense (proton) solar energetic particle (SEP) events observed at 1 AU [41,42,43]. While the association between Type III-L bursts, proton SEP events, and CMEs is now secure, the electron acceleration mechanism remains poorly understood. Two competing sites for the acceleration have been suggested: at shocks in front of a CME or in reconnection regions behind a CME.

CME Interactions and Solar Energetic Particle (SEP) Intensity: Unusually intense radio emission can occur when successive CMEs leave the Sun within 24 hours, as if CME interaction can produce enhanced particle acceleration [44,45,46]. Statistically associated with intense SEP events [47], this enhanced emission could result from more efficient acceleration due to changes in field topology, enhanced turbulence, or the direct interaction of the CMEs. The lack of radio imaging makes it difficult to determine the nature of the interaction.

II.III Lunar Atmosphere

Speculations on and attempts to measure a lunar atmosphere start as early as the 18th Century [e.g., 48,49]. Prior to the Space Age, radio astronomical measurements of lunar occultations [50] were used to suggest a tenuous atmosphere, which quickly led to the identification of various sources [51], including one still considered plausible, namely the outgassing of primordial gasses. It was also recognized that its tenuous nature meant the lunar atmosphere would be strongly influenced by its environment, e.g., exposure to the solar wind [52]. By the time of the *Apollo* missions, the major properties of the lunar atmosphere were elucidated as well as the recognition that even modest human activity could alter it substantially [53]. Reviews of the state of knowledge at the close of the *Apollo* era indicate significant advances regarding the composition, sources and sinks, and influences on the lunar atmosphere but also many remaining questions [e.g., 54,55].

Apollo Lunar Surface Experiments Package (ALSEP) measurements found a surface photoelectron layer with electron densities up to 10^4 cm^{-3} [56]. Dual-frequency radio occultation measurements from the Soviet Luna spacecraft suggest that the ionosphere's density is highly variable and can extend to significant altitudes, exceeding 10^3 cm^{-3} well above 10 km (Fig. 3). However, the interpretation of the Luna data is model dependent, as Bauer [57] concluded that they were consistent with no significant ionosphere. Exposed to both the solar and interstellar radiation fields, the lunar atmosphere is mostly ionized, and we use the terms *atmosphere* and *ionosphere* interchangeably.

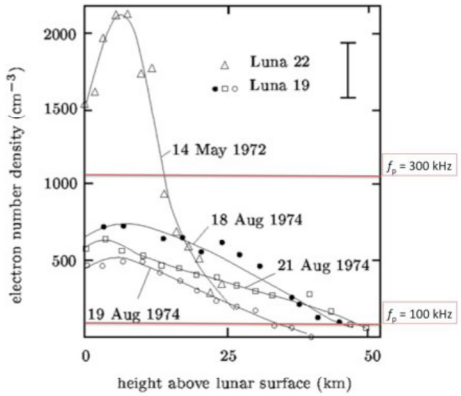

Fig. 3: Lunar ionosphere electron densities derived from radio occultation measurements with the Luna 19 and Luna 22 spacecraft [58,59]. Horizontal lines show implied plasma frequencies.

There has been a series of spacecraft-based remote sensing efforts to measure the lunar ionosphere. Pluchino et al. [61] performed dual-frequency (2.2 and 8.4 GHz) occultation observations of the SMART-1, *Cassini*, and Venus Express spacecraft, and one of the experiments on the Japanese SELENE (KAGUYA) mission used dual-frequency measurements (2.2 and 8.5 GHz) [62]. An increase in the electron density on the solar illuminated side of the Moon has been observed, consistent with expectations for a lunar ionosphere.

A significant, and acknowledged, systematic error for these (or any) spacecraft measurements is the transmission through the terrestrial ionosphere. The observational methodology is to transmit signals from the spacecraft to a ground station, with the signals passing through both the lunar and terrestrial ionospheres. With typical densities of 10^6 cm^{-3}, the magnitude of the terrestrial contribution is much larger than that of any lunar contribution. Spacecraft-based remote sensing ultimately is limited by the extent to which the (much larger) terrestrial ionospheric contribution can be estimated and removed.

Further, the density of the lunar ionosphere should vary dramatically, due to a variety of influences including the diurnal solar illumination changes, immersion in the Earth's magnetosphere, changes over a solar cycle, and even exhaust from landers. However, many of these spacecraft measurements of the lunar ionosphere suffer from relatively short mission durations, in some cases consisting of only a single epoch. The importance of such measurements is discussed in the NRC report *The Scientific Context for the Exploration of the*

Moon [63], which identified the "Lunar Environment," particularly the fact that the lunar atmosphere presents the nearest example of a surface boundary exosphere, as one of four guiding themes for science-based exploration. From this theme, the report develops a set of science goals, including "Determine the global density, composition, and time variability of the fragile lunar atmosphere before it is perturbed by further human activity." This report also notes that the Moon may continue to outgas and that the lunar atmosphere, as it is coupled to the solar wind, is a dynamic system. As such, long-term monitoring is required to understand its properties. Finally, as a surface boundary exosphere, studies of the Moon are likely to inform processes occurring on Mercury, other moons, asteroids, and potentially even Kuiper Belt objects. These themes and goals are echoed in the NRC report *Vision and Voyages for Planetary Science in the Decade 2013–2022* [64].

Determining and tracking the properties of the lunar atmosphere both robustly and over time requires a lunar-based methodology by which the atmosphere can be monitored over multiple day-night cycles. A robust, lunar surface-based method for monitoring the properties of the lunar atmosphere is relative ionospheric opacity measurements or *riometry*. This technique exploits the absorption that occurs at frequencies below the plasma frequency to determine the plasma frequency and, from that, the plasma density.

A lunar relative ionospheric opacity meter or *riometer* would measure the spectrum of a broadband reference emitter with a known spectrum observed through the lunar atmosphere. By monitoring the plasma frequency, a lunar riometer could track temporal changes in the density. The standard reference emitter is the synchrotron emission from the Milky Way Galaxy that is generated by relativistic electrons spiraling in its magnetic field. This Galactic emission has the favorable properties of being extremely well characterized, broadband, and constant in time. Riometers have been used for decades, in remote and hostile environments, for tracking the properties of Earth's ionosphere.

Finally, if the plasma frequency of the lunar atmosphere is sufficiently high, it could affect measurements of space weather and particle acceleration measurements (§II.II) by limiting the lowest frequencies accessible from the surface of the Moon.

II.IV Magnetospheric Emissions from Extrasolar Planets

The magnetic polar regions of the Earth and the solar system giant planets host intense electron cyclotron masers generated by interactions between solar wind-powered currents and planetary magnetospheric fields (Fig. 4). Empirical relations for solar system planets suggest that extrasolar planetary radio emission may be detectable [65], and the emission frequencies of some planets may be in the range relevant to Cosmic Dawn studies [e.g., 66].

The dynamo currents generating a planet's magnetic field arise from differential rotation, convection, compositional dynamics, or a combination of these in the planet's interior. Consequently, knowledge of the planetary magnetic field places constraints on a variety of planetary properties, some of which will be difficult to determine by other means.

Planetary Interiors: For the solar system planets, the composition of the conducting fluid ranges from liquid iron in the Earth's core to metallic hydrogen in Jupiter and Saturn to perhaps a brine in Uranus and Neptune. Radio detection of an extrasolar planet, combined with an estimate of the planet's mass and radius, could constrain the planet's internal composition.

Planetary rotation: The rotation of a planet imposes a periodic modulation on the radio emission, as the emission is beamed in the direction of the local magnetic field and will change if the magnetic and spin axes of the planet are not aligned. For all of the giant planets in the solar system, this modulation defines their rotation periods.

Planetary Satellites: In addition to being modulated by its rotation, Jupiter's radio emission is affected by the presence of its satellite Io, and more weakly by Callisto and Ganymede. Modulations of planetary radio emission may reveal the presence of a satellite.

Atmospheric retention: If the thermal velocity of molecules in a planet's atmosphere is sufficiently less than the planet's escape velocity, the planet will retain its atmosphere. For a planet immersed in a stellar wind, non-thermal atmospheric loss mechanisms can be important [67], as the typical stellar wind particle has a supra-thermal velocity. If directly exposed to a stellar wind, a planet's atmosphere can erode more quickly. Based on Mars Global Surveyor observations, this erosion process is thought to have been important for Mars' atmosphere and oceans [68,69].

Habitability: A magnetic field may determine the habitability of a planet by deflecting cosmic rays [e.g., 70]. In addition to its effect on the atmosphere, if the cosmic ray flux at the surface of an otherwise habitable planet is too large, it could cause cellular damage or frustrate the origin of life altogether.

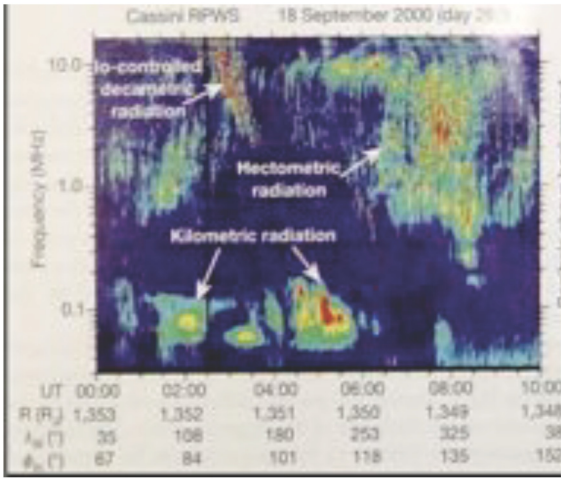

Fig. 4: Dynamic spectrum of Jovian electron cyclotron maser emission. Intensity is shown on a logarithmic color scale as a function of time (abscissa) and frequency (ordinate). Jovian emission extends as high as 40 MHz, overlapping somewhat with the frequency range relevant for Cosmic Dawn studies, and extrasolar planets may exhibit similar emissions. (The *Cassini* instrument does not operate above 16 MHz.)

Absent a direct radio detection of magnetically generated emission, evidence for extrasolar planetary magnetic fields is suggestive, but ambiguous, ranging from efforts to detect aurorally generated UV emission from "hot Jupiters" [71] to efforts to explain the inflated radii of "hot Jupiters" by Ohmic dissipation [e.g., 72] to stars showing apparently magnetically-generated star-planet interactions [73]. However, the range of estimated field strengths varies immensely, from 10% that of Jupiter to several times that of Jupiter, sometimes for the same object!

III. Lunar Surface Radio Antennas and Telescopes

Studies of the Cosmic Dawn and Dark Ages offer a significant scientific return—tracking the evolution of the Universe and the growth of the first structure over much of its first billion years—a duration of the Universe's history that will not be able to be probed in another other manner. The most powerful means of tracking this evolution is via a power spectral analysis of the highly redshifted 21 cm signal (§II.I.II), which will require a large telescope array on the far side of the Moon. We now summarize a roadmap for the development of the technical capability for such a large array, which involves a series of ever more complex and powerful antennas and arrays, culminating in a radio telescope array for Cosmic Dawn and Dark Ages studies (Table I); see also Jester & Falcke [74]. We do not discuss on-going ground-based work for studies of the Epoch of Reionization, Cosmic Dawn, and the Dark Ages (but see §§II.I.I and II.I.II), though they will clearly be extremely valuable in providing early detections, particularly at the relatively "low" redshifts of the Epoch of Reionization, and developing techniques.

	Stage	Science Motivation	Location	Dimensions / Number of Antennas	Frequency
Stage Ia	Lunar Orbiter	Cosmic Dawn	Lunar orbit	~ 1 m 1 antenna	40–120 MHz
Stage Ib	Lunar Atmosphere Probe Station	Lunar atmosphere	Near or far side	~ 10 m 1 antenna	0.1–3 MHz
	Cosmology Dipole	Cosmic Dawn	Far side	~ 1 m 1 antenna	40–120 MHz
Stage II	Radio Observatory on the Lunar Surface for Solar studies	Space weather and particle acceleration	Near or far side	~ 1 km 100 antennas	1–10 MHz
Stage III	Lunar Radio Array	Cosmic Dawn and Dark Ages	Far side	~ 10 km 10^5 antennas	20–120 MHz

Table I: Roadmap for lunar surface antennas and telescope arrays.

III.I Stage Ia: Lunar Orbiter

Early investigations into Cosmic Dawn, accessing the radio shielded zone behind the Moon and at frequencies at which terrestrial ionospheric absorption is likely to become significant, can be done on an orbiting satellite. In this concept, data would be acquired while above the far side of the Moon and downlinked to the Earth while above the near side. Such a mission has the advantage that it

allows for initial science pathfinding accessing the radio shielded zone and does not require the additional complexity of a lander. However, the need for orbital control requires on-board consumables and likely limits the duration of such a mission. One such concept for a lunar orbiter probing into Cosmic Dawn is the Dark Ages Radio Explorer (DARE, Fig. 5) [75].

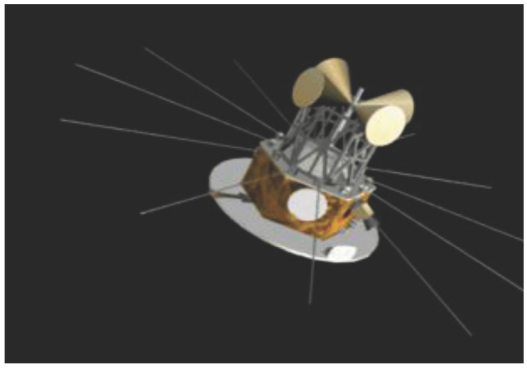

Fig. 5: Artist's conception of the Dark Ages Radio Explorer (DARE), a lunar orbiting mission for studying Cosmic Dawn.

III.II Stage Ib: Lunar Surface Antenna

On the surface of the Moon, a single antenna could be used to conduct one of two science observations, depending upon its location. A single antenna would also be a valuable technology demonstration toward a future, larger array of many antennas. This stage could proceed in parallel with a lunar orbiting mission.

If located on the near side, the antenna would serve as a monitor of the properties of the lunar ionosphere. If located on the far side, the antenna could serve as a complement to an orbiting mission. Of course, an antenna on the far side would require a means of relaying the data back to Earth, but, if conducted in conjunction with human exploration activities, such a relay satellite may be available.

An attractive technology for a lunar surface antenna (and a future array of antennas, see below) is a polyimide film-based dipole (Fig. 6). In this concept, a conductor is deposited on polyimide film, which is rolled for transport to the lunar surface and then deployed on the lunar surface simply by unrolling. Polyimide film has a long spaceflight heritage, and initial tests indicate that it is capable of significant exposure on the lunar surface [76]. A number of tests of polyimide film-based antennas have shown that they have an acceptable electrical performance (e.g., antenna feedpoint impedance as a function of frequency).

A single antenna would be a small package, possible of being carried on a lander operated either by a national space agency or by a commercial entity; the Farside Explorer is one such concept [76]. There are multiple deployment options, including an autonomous rover, a telerobotically operated rover, a propelled javelin, an inflatable, or even an astronaut laying out the antenna (Fig. 7).

Fig. 6: Polyimide film-based dipole antenna. This antenna was used in a test of its electrical performance and absorption due to the *terrestrial* ionosphere was detected. On-going work is to move the antenna testing to a more realistic lunar analog environment.

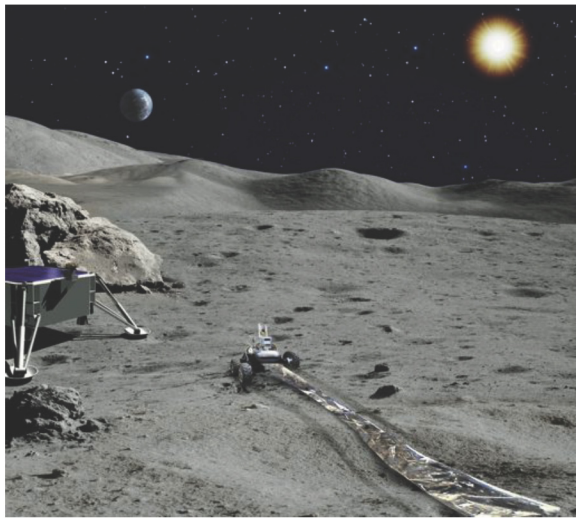

Fig. 7: Artist's conception of a single polyimide film-based dipole being deployed on the lunar surface by a rover. In this view, the dipole would be deployed on the near side for studies of the lunar ionosphere. A dipole deployed on the lunar far side could be used for studies of Cosmic Dawn that would parallel those that could be done with a lunar orbiter. Alternate deployment mechanisms have also been considered.

III.III Stage II: Radio Observatory on the Lunar Surface for Solar Studies (ROLSS)

An intermediate scale radio telescope array would be suitable for conducting solar studies, observing the radio emission from solar system planets, and potentially the radio emission from extrasolar planets. This telescope could usefully be located on the near side of the Moon because the frequencies of interest are ones for which Earth-based transmitters are partially or completely blocked by absorption from the Earth's ionosphere.

The primary requirement for such an array is that it is capable of imaging the particle acceleration and space weather events at the frequencies of interest. Current, single antenna instruments have limited imaging capabilities. In turn, the technical requirements on such an array are for it to have a number of antennas with a range of separations sufficient to deliver the required angular resolution and imaging fidelity at the frequencies of interest. The required angular resolution is approximately 2º at frequencies below 10 MHz, implying an array dimension of order 1 km (Table 1).

The Radio Observatory on the Lunar Surface for Solar Studies (ROLSS) is a concept that meets these requirements [77]. It consists of three arms, in a Y configuration, with each arm containing 16 antennas in an approximately logarithmic radial distribution from the center of the array. Antenna electronics, data acquisition, and avionics would be housed in a central electronics package at the center of the array.

Such an array obtains acceptable imaging performance. However, the initial design of a Y configuration was designed to be simple to deploy in a limited time by astronauts on the lunar surface using a crewed rover. Such a configuration also has the advantage that transmitting the signals from the antennas to the central electronics package is straightforward; the transmission lines can be run alongside or incorporated into the polyimide film supporting the dipole antennas.

Higher fidelity imaging performance likely could be obtained by distributing the dipole antennas without the restriction of three linear arms. In this scenario, the antennas could be deployed by a rover, operating either autonomously or telerobotically. Antennas could be deployed either individually or in small groups, along with the associated electronics for each, though the total number of antennas deployed (50–100) would still be required.

III.IV Stage III: Lunar Radio Telescope Array

The full power of the 21 cm cosmological signal, over the full range of cosmic epochs (redshifts), can only be exploited by making (angular) power spectral measurements of the 21 cm fluctuations (§II.I.II). The combination of angular resolution and sensitivity means that an array is the most cost-effective manner of conducting these measurements, and the array will have to be located on the far side of the Moon in order to be shielded from the intense terrestrial radio frequency interference.

As Table 1 summarizes, the resulting array dimensions are of order 10 km, with at least 10^4 antennas operating below 100 MHz. The Lunar Radio Array is a concept for such an array [78]. It will benefit immensely from the technology development provided by LAPS and ROLSS and the science pathfinding provided by ground-based telescopes and a lunar orbiter such as DARE. Further, many of the technical developments required for the LRA would benefit other NASA missions. Such technologies include low-power electronics; autonomous, low power generation; and high payload-to-rover mass ratios for rovers. Deployment of the LRA will require capable rovers, though potentially with human oversight. A complementary concept, though focused on somewhat lower frequencies, was the Very Low Frequency Array [79].

IV. Exploration Relevance

There are three primary ways that the set of science observations and associated telescopes and instruments described here are potentially relevant to human exploration efforts.

Plasma Environment and Surface Charging: There is the possibility that the lunar surface exhibits significant charging, which could be a generic property of airless bodies. Discharge or arcing of accumulated charge could cause considerable damage to electronics, particularly if connected to cables with significant linear extents. Lunar surface antennas will have to be designed to survive the plasma environment and can serve as a test bed for mitigation and electronic survival strategies.

Deployment of Packages During Operations: Lunar surface antennas have to be deployed over potentially significant distances from the electronics (~ 100 m). Concepts being developed include rovers, spring-loaded javelins, and inflatable mechanisms, all of which may have applicability to a wider range of both science and human exploration packages.

Telerobotic Operations: Astronauts deploying lunar surface antennas or arrays could test concepts for remote operations that might be applicable for future missions to near-Earth

objects (NEOs) or Mars. Burns et al. [80] describe one such mission concept, involving a crewed vehicle at the Earth-Moon Lagrange 2 point operating a rover on the far side.

Acknowledgements

The LUNAR consortium is funded by the NASA Lunar Science Institute (via Cooperative Agreement NNA09DB30A) to investigate concepts for astrophysical observatories on the Moon. The ROLSS and initial LAPS concept studies were funded by the NASA Lunar Sortie Science Opportunities (LSSO) program. The LRA concept study was funded by the NASA Advanced Strategic Mission Concept Studies program. Part of this research was carried out at the Jet Propulsion Laboratory, California Institute of Technology, under a contract with NASA.

References

[1] North American Aviation Inc., Space Information Division 1966, *Research Program on Radio Astronomy and Plasma for Apollo Applications Program Lunar Surface Missions: Final Report* (NAS8-20198)

[2] Greiner, J. M. 1967, Utilization of Crater Reflectors for Lunar Radio Astronomy, Working Group on Extraterrestrial Resources, Fifth Annual Meeting

[3] Weiler, K. W. 1986a, *Radio Astronomy from Space* (National Radio Astron. Observatory)

[4] Burns, J. O., Duric, N., Johnson, S., & Taylor, G. J. 1989, *A Lunar Far-Side Very Low Frequency Array* (NASA)

[5] Mumma, M. J., & Smith, H. J. 1990, *Astrophysics from the Moon: Proceedings of the Workshop* (Amer. Institute of Phys.: New York)

[6] Kassim, N. E., & Weiler, K. W. 1990, *Low Frequency Astrophysics from Space: Proceedings of an International Workshop* (Springer-Verlag: Berlin)

[7] Stone, R. G., Weiler, K. W., Goldstein, M. L., & Bougeret, J.-L. 2000 *Radio Astronomy at Long Wavelengths* (Amer. Geophys. Union: Washington, DC)

[8] Lester, D. F., Yorke, H. W., & Mather, J. C. 2004, "Does the Lunar Surface Still Offer Value As a Site for Astronomical Observatories?" Space Policy, 20, 99

[9] Loeb, A., & Zaldarriaga, M. 2007, "Eavesdropping on radio broadcasts from galactic civilizations with upcoming observatories for redshifted 21 cm radiation," J. Cosmol. Astronaut. Phys., 1, 20

[10] Bowman, J. D., Rogers, A. E. E., & Hewitt, J. N. 2008, "Toward Empirical Constraints on the Global Redshifted 21 cm Brightness Temperature During the Epoch of Reionization," Astrophys. J., 676, 1

[11] Rogers, A. E. E., & Bowman, J. D. 2008, "Spectral Index of the Diffuse Radio Background From 100 to 200 MHz," AJ, 136, 641

[12] Bowman, J. D., & Rogers, A. E. E. 2010a, "A first constraint on reionization from hydrogen 21-cm emission between redshifts $6<z<13$," Nature, 468, 796

[13] Bowman, J. D., & Rogers, A. E. E. 2010b, "VHF-band RFI in Geographically Remote Areas," Proc. Sci.

[14] Alexander, J. K., Kaiser, M. L., Novato, J. C., Gretna, F. R., & Weber, R. R. 1975, "Scientific instrumentation of the Radio-Astronomy-Explorer-2 satellite," A&A, 40, 365

[15] Rogers, A. E. E. 2011, "Temperature contribution of ionosphere to the sky noise spectrum," EDGES Memorandum #079; http://www.haystack.mit.edu/ast/arrays/Edges/EDGES_memos/EdgesMemo.html

[16] Milkman, P. M., McKinley, D. W. R., & Borland, M. S. 1948, "Combined Radar, Photographic and Visual Observations of the Perseid Meteor Shower of 1947," Nature, 161, 278

[17] Lazio, T. J. W., Clarke, T. E.; Lane, W. M., et al. 2010, "Surveying the Dynamic Radio Sky with the Long Wavelength Demonstrator Array," AJ, 140, 1995

[18] Fan, X., Carilli, C. L., & Keating, B. 2006, "Observational Constraints on Cosmic Reionization," ARA&A, 44, 415

[19] Shull, J. M., & Venkatesan, A. 2008, "Constraints on First-Light Ionizing Sources from Optical Depth of the Cosmic Microwave Background," Astrophys. J., 685, 1

[20] Dunkley, J., Komatsu, E., Nolta, M. R., et al. 2009, "Five-Year Wilkinson Microwave Anisotropy Probe Observations: Likelihoods and Parameters from the WMAP Data," Astrophys. J. Suppl., 180, 306

[21] National Research Council, *New Worlds, New Horizons in Astronomy and Astrophysics* (National Academies: Washington, DC)

[22] Loeb, A. 2006, "The dark ages of the Universe," Scientific Amer., 295, 46

[23] Pritchard, J. R., & Loeb, A. 2008, "Evolution of the 21cm signal throughout cosmic history," Phys. Rev. D., 78, id 103511

[24] Madau, P., Meiksin, A., & Rees, M. J. 1997, "21 Centimeter Tomography of the Intergalactic

Medium at High Redshift," Astrophys. J., 475, 429
[25] Furlanetto, S. R., Oh, S. P., & Briggs, F. H. 2006, "Cosmology at low frequencies: The 21 cm transition and the high-redshift Universe," Phys. Rep., 433, 181
[26] Pritchard, J., & Loeb, A. 2011, "21-cm Cosmology," Rep. Progress Phys., in press; arXiv:1109.6012
[27] Pritchard, J. R., & Loeb, A. 2010, "Constraining the unexplored period between the dark ages and reionization with observations of the global 21 cm signal," Phys. Rev. D., 82, 023006
[28] Furlanetto, S. R. 2006, "The global 21-centimeter background from high redshifts," MNRAS, 371, 867
[29] Harker, G. J. A., Pritchard, J. R., Burns, J. O., & Bowman, J. D. 2012, "An MCMC approach to extracting the global 21-cm signal during the cosmic dawn from sky-averaged radio observations," MNRAS, 419, 1070
[30] Bowman, J. D., & Rogers, A. E. E. 2010a, "A first constraint on reionization from hydrogen 21-cm emission between redshifts 6<z<13," Nature, 468, 796
[31] Parsons, A. R., Backer, D. C., Foster, G. S., et al. "The Precision Array for Probing the Epoch of Re-ionization: Eight Station Results," AJ, 139, 1468
[32] Paciga, G. Chang, T.-C., Gupta, Y., et al. "The GMRT Epoch of Reionization experiment: a new upper limit on the neutral hydrogen power spectrum at $z \approx 8.6$," MNRAS, 413, 1174
[33] Holzbauer, L. N., & Furlanetto, S. R. 2012, "Fluctuations in the High-Redshift Lyman-Werner and Lyα Radiation Backgrounds," MNRAS, 419, 718
[34] Dalal, N., Pen, U.-L., & Seljak, U. 2010, "Large-Scale BAO Signatures of the Smallest Galaxies," J. Cosmol. Astropart. Phys., 11, 7
[35] Leblanc, Y., Dulk, G. A., & Bougeret, J.-L. 1998, "Tracing the Electron Density from the Corona to 1 AU," Solar Phys., 183, 165
[36] Mann, G., Jansen, F., MacDowall, R. J., Kaiser, M. L., & Stone, R. G. 1999, "A heliospheric density model and type III radio bursts," A&A, 348, 614
[37] Bougeret, J.-L., Kaiser, M. L., Kellogg, P. J., et al. 1995, "Waves: The Radio and Plasma Wave Investigation on the Wind Spacecraft," Space Sci. Rev., 71, 231
[38] Bale, S. D., Reiner, M. J., Bougeret, J.-L., et al. 1999, "The Source Region of an Interplanetary Type II Radio Burst," Geophys. Res. Lett. 26, 1573
[39] Holman, G. D., & Pesses, M. E. 1983, "Solar type II radio emission and the shock drift acceleration of electrons," Astrophys. J., 267, 837
[40] Mann, G., & Luehr, H. 1994, "Electron acceleration at quasi-parallel shocks in the solar corona and its signature in solar Type II radio bursts," Astrophys. J. Suppl., 90, 577
[41] Cane, H. V., Erickson, W. C., & Prestage, N. P. 2002, "Solar Flares, Type III Radio Bursts, Coronal Mass Ejections, and Energetic Particles," JGR (Space Physics), 107(A10), SSH 14-1
[42] Lara, A., Gopalswamy, N., Nunes, S., Muñoz, G., & Yashiro, S. 2003, "A Statistical Study of CMEs Associated with Metric Type II Bursts," Geophys. Res. Lett., 30(12), SEP 4-1
[43] MacDowall, R. J., Lara, A., Manoharan, P. K., et al. 2003, "Long-duration Hectometric Type III Radio Bursts and Their Association with Solar Energetic Particle (SEP) Events," Geophys. Res. Lett., 30(12), SEP 6-1
[44] Gopalswamy, N., Yashiro, S., Kaiser, M. L., Howard, R. A., & Bougeret, J.-L. 2001, "Radio Signatures of Coronal Mass Ejection Interaction: Coronal Mass Ejection Cannibalism?" Astrophys. J., 548, L91
[45] Gopalswamy, N., Yashiro, S., Kaiser, M. L., Howard, R. A., & Bougeret, J.-L. 2002, "Interplanetary Radio Emission due to Interaction Between Two Coronal Mass Ejections," Geophys. Res. Lett., 29(8), 106-1
[46] Richardson, I. G., Lawrence, G. R., Haggerty, D. K., Kucera, T. A., & Szabo, A. 2003, "Are CME `interactions' really important for accelerating major solar energetic particle events?" Geophys. Res. Lett., 30, 120000
[47] Gopalswamy, N., Yashiro, S., Krucker, S., Stenborg, G., & Howard, R. A. 2004, "Intensity Variation of Large Solar Energetic Particle Events Associated with Coronal Mass Ejections," JGR (Space Physics), 109(A12), A12105
[48] Schroeter, J. J. 1792, "Observations on the Atmospheres of Venus and the Moon, Their Respective Densities, Perpendicular Heights, and the Twi-Light Occasioned by Them," Philos. Trans. R. Soc. London, 82, 309
[49] Challis, J. 1863, "On the Indications by Phenomena of Atmospheres to the Sun, Moon and Planets," MNRAS, 23, 231
[50] Elsmore, B. 1957, "Radio observations of the lunar atmosphere," Philos. Magazine, 2, 1040
[51] Edwards, W. F., & Borst, L. B. 1958, "Possible Sources of a Lunar Atmosphere," Science, 127, 325

[52] Herring, J. R., & Licht, A. L. 1959, "Effect of the Solar Wind on the Lunar Atmosphere," Science, 130, 266
[53] Milford, S. N., & Pomilla, F. R. 1967, "A Diffusion Model for the Propagation of Gases in the Lunar Atmosphere," JGR, 72, 4533
[54] Johnson, F. S. 1971, "Lunar Atmosphere," Rev. Geophys. Space Phys., 9, 813
[55] Hodges, R. R., Hoffman, J. H., & Johnson, F. S. 1974, "The Lunar Atmosphere," Icarus, 21, 415
[56] Reasoner, D. L., & O'Brien, B. J. 1972, "Measurement on the lunar surface of impact-produced plasma clouds," JGR, 77, 1292
[57] Bauer, S. J. 1996, "Limits to a Lunar Ionosphere," Sitzungsberichte und Anzeiger, Abt. 2, 133, 17
[58] Vyshlov, A. S. 1976, "Preliminary results of circumlunar plasma research by the Luna 22 spacecraft," Space Research, XVI, Proc. of Open Meetings of Workshop Groups of Physical Sciences (Akademie-Verlag) 945
[59] Vyshlov, A. S., & Savich, N. A. 1978, "Observations of radio source occultations by the Moon and the nature of the plasma near the Moon," Cosmic Res., 16 (transl. Kosmicheskie Issledovaniya, 16), 551
[60] Rennilson, J. J., & Criswell, D. R. 1974, "Surveyor Observations of Lunar Horizon-Glow," Moon, 10, 121
[61] Pluchino, S., Schillirò, F., Salerno, E., Pupillo, G., Maccaferri, G., & Cassaro, P. 2008, "Radio Occultation Measurements of the Lunar Ionosphere," Memorie Soc. Astron. Italiana Suppl., 12, 53
[62] Imamura, T., Iwata, T., Yamamoto, Z., et al. 2008, "Studying the Lunar Ionosphere with SELENE Radio Science Experiment," American Geophysical Union, #P51D-04
[63] National Research Council, *New Scientific Context for the Exploration of the Moon* (National Academies: Washington, DC)
[64] National Research Council, *Vision and Voyages for Planetary Science in the Decade 2013–2022* (National Academies: Washington, DC)
[65] Farrell, W. M., Desch, M. D., & Zarka, P. 1999, "On the possibility of coherent cyclotron emission from extrasolar planets," JGR, 104, 14025
[66] Lazio, T. J. W., Shankland, P. D., Farrell, W. M., & Blank, D. L. 2010, "Radio Observations of HD 80606 Near Planetary Periastron," AJ, 140, 1929
[67] Shizgal, B. D., & Arkos, G. G. 1996, "Nonthermal Escape of the Atmospheres of Venus, Earth, and Mars," Rev. Geophys., 34, 483
[68] Lundin, R., Barabash, S., Andersson, H., et al. 2004, "Solar Wind-Induced Atmospheric Erosion at Mars: First Results from ASPERA-3 on Mars Express," Science, 305, 1933
[69] Crider, D. H., Epley, J., Brain, D. A., et al. 2005, "Mars Global Surveyor Observations of the Halloween 2003 Solar Superstorm's Encounter with Mars," JGR, 110, A09S21
[70] Griessmeier, J.-M., Stadelmann, A., Motschmann, U., et al. 2005, "Cosmic Ray Impact on Extrasolar Earth-Like Planets in Close-in Habitable Zones," Astrobiology, 5, 587
[71] France, K., Stocke, J. T., Yang, H., et al. 2010, "Searching for Far-ultraviolet Auroral/Dayglow Emission from HD 209458b," Astrophys. J., 712, 1277
[72] Batygin, K., & Stevenson, D. J. 2010, "Inflating Hot Jupiters With Ohmic Dissipation," Astrophys. J., 714, L238
[73] Shkolnik, E., Bohlender, D. A., Walker, G. A. H., & Collier Cameron, A. 2008, "The On/Off Nature of Star-Planet Interactions," Astrophys. J., 676, 628
[74] Jester, S., & Falcke, H. 2009, "Science with a lunar low-frequency array: From the dark ages of the Universe to nearby exoplanets," New Astron. Rev., 53, 1
[75] Burns, J. O., Lazio, J., Bale, S., et al. 2012, "Probing the first stars and black holes in the early Universe with the Dark Ages Radio Explorer (DARE)," Adv. Space Res., 49, 433
[76] Mimoun, D., Wieczorek, M. A., Alkalai, L., et al. 2011, "Farside explorer: unique science from a mission to the farside of the moon," Exp. Astron., DOI 10.1007/s10686-011-9252-3
[77] Lazio, T. J. W., MacDowall, R. J., Burns, J. O., et al. 2011, "The Radio Observatory on the Lunar Surface for Solar studies," Adv. Space Res., 48, 1942
[78] Lazio, J., Carilli, C., Hewitt, J., Furlanetto, S., & Burns, J. 2009, "The lunar radio array (LRA)," in UV/Optical/IR Space Telescopes: Innovative Technologies and Concepts IV, Proc. SPIE, eds. H. A. MacEwen & J. B. Breckinridge, Vol. 7436, 74360I-11
[79] "Very Low Frequency Array on the Lunar Far Side," Very Low Frequency Astronomy Study Team, 1997, European Space Agency, publication ESA SCI(97)2
[80] Burns, J. O., Kring, D., Norris, S., Hopkins, J., Lazio, J., & Kasper, J. 2012, "A Lunar L2-Farside Exploration and Science Mission with the Orion Multi-Purpose Crew Vehicle and a Teleoperated Lander/Rover," Global Space Exploration Conference 2012, Washington, DC